

Constraints on Primordial Black Hole Dark Matter from the Stochastic Gravitational-Wave Background

Gokdeniz Baydar*

University of Minnesota, Twin Cities

(Dated: April 20, 2025)

This work investigates the contribution of primordial black hole (PBH) binaries to the stochastic gravitational-wave background (SGWB) using data from the LIGO–Virgo–KAGRA (LVK) collaboration. A Bayesian inference framework is employed to model the PBH population with a log-normal mass distribution, incorporating early binary formation and suppression effects from environmental interactions such as tidal disruptions and clustering. Observational limits from the LVK O1–O3 runs are used to constrain the PBH dark matter fraction. The results place stringent upper bounds on PBH abundances in the $0.05\text{--}10 M_{\odot}$ mass range and demonstrate that suppression effects significantly reduce the allowed parameter space. These refined constraints are essential for assessing the role of PBHs as dark matter candidates and emphasize the importance of future observations with instruments such as LIGO O4, LISA, and DECIGO.

Keywords: Primordial black holes, stochastic gravitational-wave background, LIGO, suppression effects

I. INTRODUCTION

Gravitational waves (GWs), ripples in spacetime predicted by Einstein’s General Theory of Relativity, have created a new frontier in cosmology. The first direct detection of GWs by the LIGO–Virgo–Kagra Collaboration (LVK) in 2015 made direct investigation of this phenomenon possible. Among various potential sources, primordial black holes (PBHs) have emerged as candidates contributing to the stochastic gravitational-wave background (SGWB). SGWB is a pervasive and continuous GW signal arising from numerous unresolved sources distributed throughout the universe.

Primordial black holes, theoretically proposed in 1966 by Yakov Zeldovich and Igor Novikov, are thought to form from the collapse of large curvature perturbations generated during inflation in the early universe [3, 4]. Unlike stellar-mass black holes originating from collapsed massive stars, PBHs span an extensive mass range and can form independently of stellar evolutionary processes. Their versatile mass spectrum, potentially ranging from subatomic-scale black holes to supermassive ones, makes PBHs also a viable candidate for dark matter. Thus, constraining their abundance and mass distribution is crucial, not only for GW astrophysics but also for understanding cosmological models and the nature of dark matter.

The SGWB generated by PBHs predominantly arises from their formation mechanisms, early-universe interactions, and binary coalescence. PBH binaries can form dynamically through gravitational capture events in dense environments or through primordial gravitational decoupling during the universe’s radiation-dominated era [2, 8]. Each formation pathway leads to distinct observable signatures in the SGWB, represented by its spectral shape and amplitude. As a result, careful analysis of SGWB data from current and future GW observatories offers constraints on PBH populations.

The LIGO collaboration has placed upper bounds on the SGWB in the 20–100 Hz frequency band using data from their first three observing runs (O1–O3). This has limited the contribution of PBHs to the total dark matter abundance [1]. Interpreting these constraints requires a framework that includes the PBH mass distribution, binary formation channels, redshift evolution, and suppression effects [2, 5].

This study adopts a minimal modeling approach based on a log-normal PBH mass function. The GW energy spectrum $\Omega_{\text{PBH}}(f)$ is computed by integrating the merger rate over redshift and mass, including relevant suppression factors. The predictions from this model are then rigorously compared with the LIGO upper limits to constrain the dark matter fraction of PBHs, denoted as f_{PBH} .

The computational framework used here is based on the existing methodologies developed by Töre Boybeyi, who also supervised this project. By using several statistical methodologies, including Bayesian inference and Markov Chain Monte Carlo (MCMC) simulations, this work quantitatively assesses constraints on the PBH fraction of dark matter. Key results include a posterior contour plot in the $\mu\text{--}f_{\text{PBH}}$ plane, portraying the allowed parameter space, and a constraint curve illustrating upper limits on f_{PBH} across different PBH masses [1, 8].

This analysis aims to improve our understanding of PBHs and the parameters that constrain them, while also helping to guide observational strategies and data-analysis efforts for future gravitational-wave detectors.

II. THEORETICAL FRAMEWORK

The abundance and mass distribution of PBHs are key to cosmological models [3, 4]. The present-day fraction of dark matter composed of PBHs, $f_{\text{PBH}}(M)$, can be calculated from the initial mass fraction, $\beta(M)$, which quantifies the fraction of the mass of the universe collapsing into PBHs at formation. The relation between these two fractions is expressed as follows:

* Correspondence email address: bayda002@umn.edu

$$f_{\text{PBH}}(M) = 2.7 \times 10^8 \left(\frac{\gamma}{0.2}\right)^{1/2} \left(\frac{g_{*,\text{form}}}{10.75}\right)^{-1/4} \left(\frac{M}{M_\odot}\right)^{-1/2} \beta(M) \quad (1)$$

Here, γ represents the collapse efficiency factor, typically around 0.2 for standard formation scenarios, and $g_{*,\text{form}}$ is the effective number of relativistic degrees of freedom at the epoch of PBH formation. The initial mass fraction, $\beta(M)$, can be approximated by:

$$\beta(M) \approx \frac{\gamma}{\sqrt{2\pi} \nu(M)} \exp\left[-\frac{\nu(M)^2}{2}\right], \quad (2)$$

where $\nu(M) \equiv \delta_{\text{th}}/\sigma_M$ represents the ratio of the threshold density contrast δ_{th} required for collapse, to the variance of the density perturbations σ_M at a mass scale M [10]. This parameter directly influences the likelihood of collapse and thus the initial abundance of PBHs.

To characterize PBH populations, a log-normal mass distribution is used and given by:

$$\psi(m) = \frac{1}{\sqrt{2\pi}\sigma m} \exp\left(-\frac{(\ln m - \ln \mu)^2}{2\sigma^2}\right), \quad (3)$$

where μ is the central mass around which PBH masses cluster, and σ defines the width of the distribution. This form naturally emerges from enhanced curvature perturbations in numerous inflationary models [4, 6]. Its shape allows for both narrow and broad mass spectra, making it a flexible tool for exploring a wide range of formation scenarios. In contrast, a monochromatic mass function in which all PBHs have the same mass is a highly idealized case. Although this method is much more simplistic, it often leads to overly sharp constraints which do not reflect complex, extended mass distributions predicted by realistic PBH formation models [1, 8].

PBHs predominantly form binaries through two principal channels: early-universe gravitational decoupling and late-time dynamical interactions within dark matter halos. The merger rate of PBH binaries, defined as the number of mergers per unit volume and unit time, significantly impacts the stochastic gravitational-wave background (SGWB). It can be mathematically expressed as:

$$\frac{dR_{E2}}{d \ln m_1 d \ln m_2} \approx 1.6 \times 10^6 \text{ Gpc}^{-3} \text{ yr}^{-1} f_{\text{PBH}}^{53/37} \left(\frac{M}{M_\odot}\right)^{-32/37} \times \left(\frac{t}{t_0}\right)^{-34/37} \eta^{-34/37} S_1 S_2 \psi(m_1) \psi(m_2) \quad (4)$$

In this formula, $M = m_1 + m_2$ represents the total binary mass, $\eta = m_1 m_2 / (m_1 + m_2)^2$ is the symmetric mass ratio, and t is the cosmic time with t_0 being the current age of the Universe. The suppression factors S_1 and S_2 account for the disruption of PBH binaries. The factor S_1 models binary disruption caused by matter fluctuations, while S_2 captures the disruption due to early PBH clustering from initial Poisson fluctuations when PBHs are abundant [1, 2].

$$S_1 \approx 1.42 \left[\frac{\langle m^2 \rangle / \langle m \rangle^2}{\bar{N} + C} + \frac{\sigma_M^2}{f_{\text{PBH}}^2} \right]^{-21/74} e^{-\bar{N}}, \quad (5)$$

$$S_2 \approx \min\left(1, 9.6 \times 10^{-3} f_{\text{PBH}}^{-0.65} e^{(0.03 \ln^2 f_{\text{PBH}})}\right). \quad (6)$$

Late-time binary formation through halo-based capture provides a secondary contribution and is characterized by [2]:

$$\frac{dR_{L2}}{d \ln m_1 d \ln m_2} \approx 3.4 \times 10^{-6} \text{ Gpc}^{-3} \text{ yr}^{-1} f_{\text{PBH}}^2 \left(\frac{\sigma_v}{\text{km/s}}\right)^{-11/7} \times \eta^{-5/7} \delta_{\text{eff}} \psi(m_1) \psi(m_2) \quad (7)$$

Here, δ_{eff} describes the effective halo density contrast, and σ_v is the characteristic velocity dispersion within dark matter halos.

Finally, the GW energy density can initially be defined as:

$$\Omega_{\text{GW}}(f) = \frac{1}{\rho_c} \frac{d\rho_{\text{GW}}}{d \ln f}. \quad (8)$$

This equation can now be extended by including the contributions from merging PBH binaries, leading to this full expression [1]:

$$\Omega_{\text{GW}}(f) = \frac{f}{\rho_{c,0}} \int_0^{z_{\text{max}}} dz \int d \ln m_1 d \ln m_2 \frac{p(m_1)p(m_2)}{(1+z)H(z)} \times \frac{d^2 R}{d \ln m_1 d \ln m_2}(z, m_1, m_2) \frac{dE_{\text{GW}}}{df_r} \quad (9)$$

where $\rho_{c,0}$ is the current critical density of the Universe, $H(z)$ the Hubble parameter, and dE_{GW}/df_r the GW energy emitted by the spectrum per merger event in the source frame. The integration of this equation allows for comparison with empirical constraints from GW detectors such as LVK [8, 10].

III. COMPUTATIONAL METHODS

In order to test this theoretical framework against GW observations, a comprehensive computational pipeline was used. This computational framework specifically computes the SGWB arising from PBH binary mergers by combining Monte Carlo sampling methods, semi-analytical integrations, and empirical gravitational wave constraint data from the LVK collaboration.

Initially, the PBH mass function is defined. Then, a log-normal mass distribution parameterized by a central mass μ and width σ is adopted. These two parameters, along with the overall PBH fraction of dark matter, f_{PBH} , and the contributions from the astrophysical background, Ω_{cbc} , form the parameter space explored through Bayesian inference techniques. The analysis uses the Bayesian inference library `bilby` to utilize the Markov Chain Monte Carlo (MCMC) algorithm provided by the `emcee` sampler.

Log-uniform priors were assigned to all model parameters to reflect the wide uncertainty in their values and to ensure unbiased exploration across several orders of magnitude. The prior distributions and their corresponding ranges are summarized in Table I.

Parameter	Prior Type	Range
$\mu [M_{\odot}]$	LogUniform	10^{-2} to 120
σ	LogUniform	10^{-2} to 10^0
f_{PBH}	LogUniform	10^{-5} to 1
Ω_{cbc}	LogUniform	10^{-10} to 10^{-7}

Table I. Log-uniform prior distributions used in the Bayesian inference.

A critical component of the computational framework is the construction of the likelihood function. This is implemented via a custom `PBHModel` class, which computes the predicted SGWB spectrum $\Omega_{\text{GW}}(f)$ and compares it to the 95% upper limits published by the LVK Collaboration from the O1–O3 observing runs. This comparison is performed throughout the frequency range in the observational band, with a particular focus around ~ 25 Hz where the detectors are most sensitive. The likelihood penalizes models that exceed observational bounds, effectively constraining the parameter space. Formally, the log-likelihood is evaluated as

$$\log \mathcal{L} = -\frac{1}{2} \sum_i \left(\frac{\Omega_{\text{GW}}(f_i) - \Omega^{\text{UL}}(f_i)}{\sigma(f_i)} \right)^2,$$

where $\Omega^{\text{UL}}(f_i)$ denotes the observed upper limit and $\sigma(f_i)$ is an effective uncertainty scale. In the absence of a detected SGWB signal, this likelihood acts as a conservative filter, ruling out models that are inconsistent with current bounds.

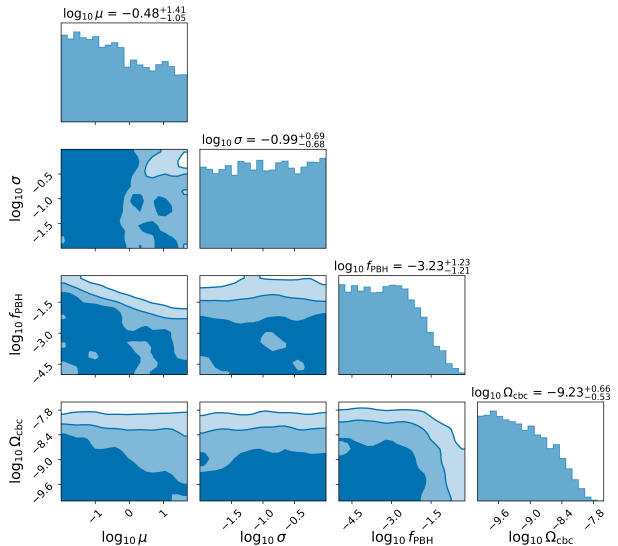
To interpret and visualize the statistical results of the Bayesian analysis, log-scaled corner plots are used. These graphs provide a detailed representation of the correlations and constraints of the parameters μ , σ , and f_{PBH} . Furthermore, two-dimensional density estimates are produced in the μ – f_{PBH} plane as a contour plot to visualize the credible parameter regions and directly compare with the existing observational limits from the LVK data. In addition, a complementary approach is used by fixing the distribution parameters (μ and σ) and systematically calculating the maximum allowed f_{PBH} at each mass scale.

The computational framework is implemented in Python and is organized into modules for mass functions, merger rates, suppression effects, and likelihood evaluations. A configuration system enables quick switching between modeling scenarios, while input datasets, including LVK constraints and PBH limits, are dynamically loaded during execution. This setup enables efficient exploration of PBH parameter space and refines dark matter constraints using gravitational-wave observations.

IV. RESULTS AND DISCUSSION

The analysis constrains PBH populations with a log-normal mass distribution, focusing on the parameters (μ, σ), f_{PBH} , and the astrophysical background Ω_{cbc} . The log-scaled corner plots obtained from the LVK O1–O3 SGWB data are shown below.

Posterior Distributions of Log-Scaled PBH Parameters (With no Suppression Applied)



Posterior Distributions of Log-Scaled PBH Parameters (With Suppression Applied)

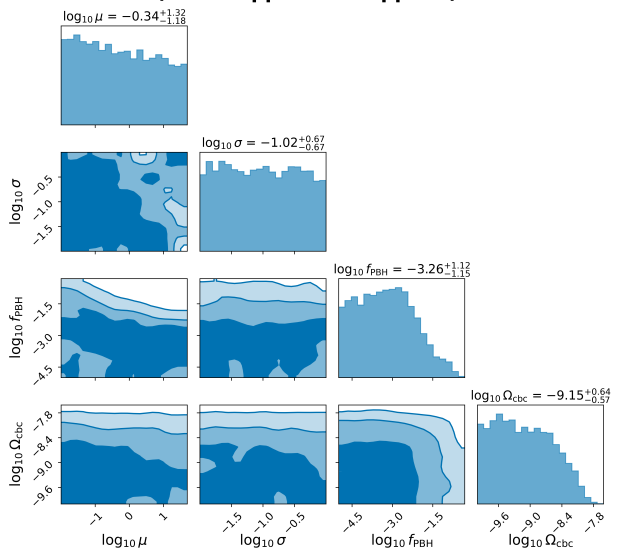


Figure 1. Corner plots showing log-scaled posterior distributions for the parameters, without suppression (top) and with suppression (bottom).

The log-scaled corner plots (Figure 1) illustrate parameter correlations and posterior distributions for ($\mu, \sigma, f_{\text{PBH}}, \Omega_{\text{cbc}}$) with and without suppression. These plots highlight the constraints placed by current observational data, clearly showing how including suppression effects significantly narrows the viable parameter space.

A concise summary of the estimated best-fit parameter values obtained from our Bayesian inference analysis is provided in Table II:

Parameter	Without Suppression	With Suppression
$\mu [M_{\odot}]$	0.33164	0.46184
σ	0.10340	0.09556
f_{PBH}	5.84×10^{-4}	5.50×10^{-4}
Ω_{cbc}	5.938×10^{-10}	6.999×10^{-10}

Table II. Best-fit parameter estimates from Bayesian inference analysis for suppressed and unsuppressed binary formation scenarios.

The values of the best-fit parameters for the suppressed and unsuppressed binary formation scenarios are summarized in Table II. The central mass μ is found to be in the sub-solar range having values around $0.33 M_{\odot}$ for the unsuppressed case and $0.46 M_{\odot}$ for the suppressed case. These results suggest that, if PBHs contribute to the dark matter content, their masses are likely concentrated around these intermediate scales. The width σ of the log-normal distribution remains relatively narrow (~ 0.1), indicating a tight clustering around the central mass rather than a broader mass spread. The inferred dark matter fractions f_{PBH} are small, approximately 5×10^{-4} in both scenarios, reaffirming that only a subdominant PBH contribution is allowed by current SGWB limits. Finally, the values of Ω_{cbc} are of the order 10^{-10} , consistent with expectations for the residual astrophysical binary background. Overall, these results demonstrate the strong constraining power of SGWB observations on PBH dark matter scenarios.

Figure 2 presents the joint posterior distributions of $\log_{10}(\mu)$ and $\log_{10}(f_{\text{PBH}})$, constructed using a smooth kernel density estimate (KDE) method. Credible regions corresponding to confidence levels 30%, 68%, 95%, and 99.7% are indicated, with the cyan dashed curve representing the LIGO upper limit. In both suppression and non-suppression scenarios, the posteriors favor low f_{PBH} values across a range of μ between ~ 0.05 and $10 M_{\odot}$. The suppression model leads to a slightly more concentrated distribution, indicating that early binary disruption mechanisms tighten the allowed parameter space. In contrast, the unsuppressed case exhibits broader credible regions, especially at higher masses. The posterior density stays well below the LIGO limit in both cases, confirming the strength of the constraints from stochastic GW observations.

Figure 3 shows the predicted f_{PBH} values required to match the LVK SGWB constraint at 25 Hz, compared to the upper limits. The predicted curves for both suppression and non-suppression binary formation scenarios lie several orders of magnitude below the observational bounds across the entire PBH mass range. This confirms that the parameter spaces explored here are consistent with existing SGWB observations. The close overlap between the suppression and non-suppression predictions also indicates that suppression effects have a relatively small impact on the allowed f_{PBH} values in this frequency regime.

The results broadly agree with previous studies [2, 7], but demonstrate tighter constraints due to the inclusion of comprehensive suppression modeling.

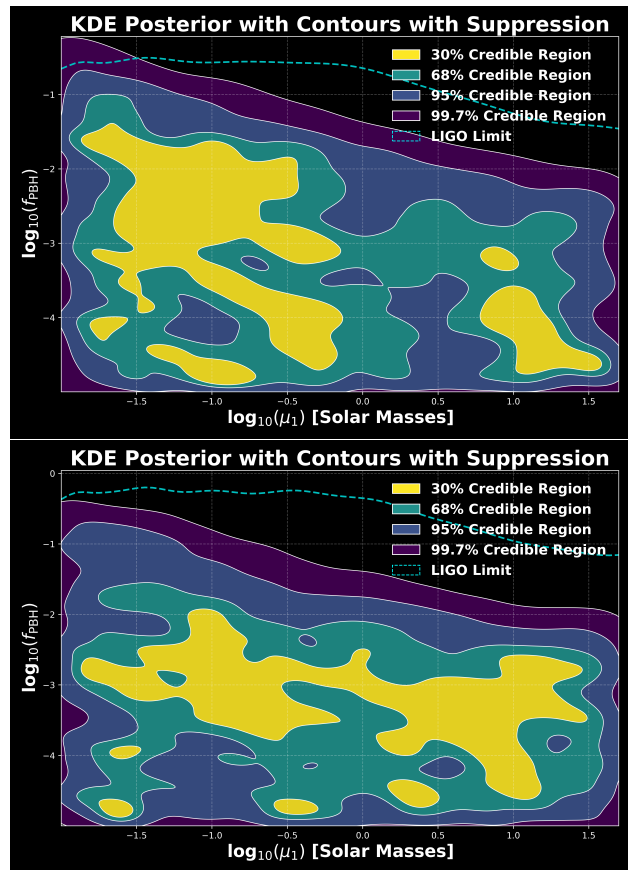


Figure 2. Kernel Density Estimate (KDE) plots illustrating credible regions without suppression (top) and with suppression (bottom).

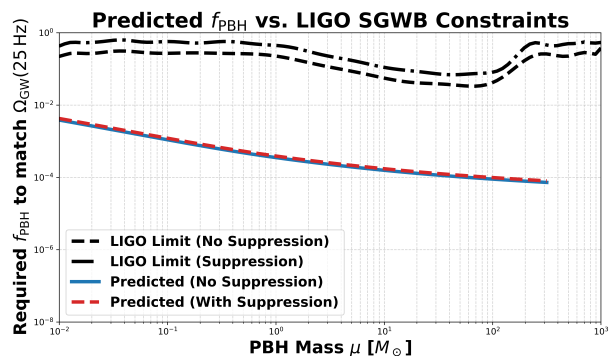


Figure 3. Exclusion curves for PBH dark matter fraction, comparing suppressed and unsuppressed models.

The inferred posterior distributions overlap with mass ranges predicted by PBH formation scenarios involving phenomena such as the QCD phase transition [6], although the corresponding dark matter fractions remain significantly below unity.

In conclusion, the analysis strongly suggests that PBHs within the mass range 0.05 – $10 M_{\odot}$ cannot constitute the entire dark matter under current GW background constraints. However, a subdominant PBH component remains plausible, particularly when environmental suppression effects are considered. These results lay the foundation for future studies based on data from the LIGO O4 observation run.

V. CONCLUSION

Bayesian inference results indicate that primordial black holes (PBHs) in the $0.05\text{--}10 M_{\odot}$ mass range can account for only a small fraction of dark matter. Suppression effects significantly reduce the predicted merger rates and tighten the resulting constraints. Although broadly consistent with previous studies, the inclusion of suppression mechanisms provides a more

refined exclusion of PBH scenarios.

This framework supports future extensions to explore alternative PBH mass distributions, spin dynamics, and formation channels. Sensitivity improvements from LIGO O4 and future missions such as LISA and DECIGO are expected to further tighten constraints, solidifying SGWB measurements as a powerful probe of dark matter and early-universe physics.

-
- [1] Boybeyi, T., Clesse, S., Kuroyanagi, S., & Sakellariadou, M. Search for a gravitational wave background from primordial black hole binaries using data from the first three LIGO-Virgo-KAGRA observing runs. *arXiv* **2412.18318** (2024). <https://arxiv.org/abs/2412.18318>
 - [2] Raidal, M., Vaskonen, V., & Veermäe, H. Formation of primordial black hole binaries and their merger rates. *arXiv* **2404.08416** (2024). <https://arxiv.org/abs/2404.08416>
 - [3] Escrivá, A., Kuhnel, F., & Tada, Y. Primordial Black Holes. *arXiv* **2211.05767** (2025). <https://arxiv.org/abs/2211.05767>
 - [4] Carr, B., & Kuhnel, F. Primordial Black Holes as Dark Matter Candidates. *arXiv* **2110.02821** (2022). <https://arxiv.org/abs/2110.02821>
 - [5] Escrivá, A., Germani, C., & Sheth, R. K. Analytical thresholds for black hole formation in general cosmological backgrounds. *arXiv* **2007.05564** (2020). <https://arxiv.org/abs/2007.05564>
 - [6] Inomata, K., Kawasaki, M., Mukaida, K., & Yanagida, T. K. Double inflation as a single origin of primordial black holes for all dark matter and LIGO observations. *arXiv* **1711.06129** (2019). <https://arxiv.org/abs/1711.06129>
 - [7] Clesse, S., & García-Bellido, J. Detecting the gravitational wave background from primordial black hole dark matter. *arXiv* **1812.11011** (2020). <https://arxiv.org/abs/1812.11011>
 - [8] Iovino, A. J. Cosmic Whispers of the Early Universe: Gravitational Waves and Dark Matter from Primordial Black Holes. Ph.D. Thesis, Sapienza University of Rome (2025). *arXiv* **2501.03065**. <https://arxiv.org/abs/2501.03065>
 - [9] Ali-Haïmoud, Y., Kovetz, E. D., & Kamionkowski, M. Merger rate of primordial black-hole binaries. *arXiv* **1709.06576** (2017). <https://arxiv.org/abs/1709.06576>
 - [10] Sasaki, M., Suyama, T., Tanaka, T., & Yokoyama, S. Primordial black holes—perspectives in gravitational wave astronomy. *arXiv* **1801.05235** (2018). <https://arxiv.org/abs/1801.05235>